

## Structural Diversity of Lithium Neopentoxide Compounds

Timothy J. Boyle,\* Todd M. Alam, Kelly P. Peters, and Mark A. Rodriguez

Advanced Materials Laboratory, Sandia National Laboratories, 1001 University Boulevard, SE, Albuquerque, New Mexico 87105

Received June 19, 2001

The reaction of  $\text{LiN}(\text{SiMe}_3)_2$  with 1 equiv of  $\text{HOCH}_2\text{CMe}_3$  (HONep) in toluene led to the formation of  $[\text{Li}(\mu_3\text{-ONep})]_8$  (**1**). The complex adopts a novel dual-edge fused hexagon–square prismatic structure with a  $C_{2v}$  axis of rotation that relates the top and bottom eight-membered rings. Substituting the noncoordinating solvent toluene for a Lewis basic solvent (THF or py) led to the isolation of compounds of the general formula  $[\text{Li}(\mu_3\text{-ONep})]_4(\text{solv})_3$ , where solv = THF (**2**) or py (**3**). The cube structures of **2** and **3** have one Li which is not solvated because of steric crowding of the ONep ligands. Multinuclear solid-state ( $^6\text{Li}$ ,  $^7\text{Li}$ , and  $^{13}\text{C}$ ) MAS and solution-state ( $^1\text{H}$ ,  $^7\text{Li}$ , and  $^{13}\text{C}$ ) NMR studies were undertaken to verify the identity of the bulk powder and to determine the solution behavior of these compounds.

## Introduction

It has been reported that Li-containing complexes aggregate, yielding  $\sim 12$  general structural types.<sup>1–3</sup> The factors that determine the final structure of these Li species have been attributed to the choice of solvent (Lewis basicity) used during their synthesis, the electron-donating ability of the  $\alpha$  atom of the ligand (C, N, O, or X), the bonding ability of the ligand (mono-, bi-, tri-, or polydentate), or the steric bulk and number of pendant hydrocarbon chains ( $-\text{X}$ ,  $-\text{OR}$ ,  $-\text{NR}_2$ , or  $-\text{CR}_3$ ).<sup>1–3</sup> We are interested in metal alkoxides as precursors to ceramic materials. In particular, several of our efforts have focused on generating “single-source” precursors.<sup>3–6</sup> One method to realize the synthesis of mixed-metal alkoxide species is through a metathesis route that often involves lithium alkoxides.<sup>3–5</sup> To fully exploit this method, it is necessary to identify the structure of the starting precursors; however, few  $[\text{Li}(\text{OR})]_n$  have been fully characterized.<sup>3</sup>

We recently reported on the synthesis and characterization of a series of lithium aryloxy species,  $[\text{Li}(\text{OAr})]_n$  ( $\text{OC}_6\text{H}_5\text{-}n$  (2,6-R)<sub>n</sub>, where  $n = 1$  or 2 and R = H, Me, CHMe<sub>2</sub>, or CMe<sub>3</sub>).<sup>3</sup> When these compounds were synthesized in the presence of THF, they were found to adopt hexagonal prisms, cubes, and hexagon structure types of  $[\text{Li}(\text{OAr})(\text{THF})_x]_n$  ( $n = 6, 4$ , or 3,  $x = 1$ ;  $n = 2$ ,  $x = 2$  or 1) and in the presence of py those of  $[\text{Li}(\text{OAr})(\text{py})_x]_2$  ( $x = 1$  or 2).<sup>3</sup> Additional structural arrangements were also noted in this study, and while these were new

compounds, the majority of structures were in line with the existing structural variations already observed.<sup>1–3</sup> Parts a–d of Figure 1 schematically illustrate the variations of squares and hexagons that were observed for these compounds. The majority of simple lithium alkoxide compounds that have been characterized without the use of a coordinating solvent adopt hexanuclear geometries.<sup>1–3</sup> Two exceptions are polymeric  $[\text{Li}(\text{OME})]_\infty$ <sup>7,8</sup> and dinuclear  $[\text{Li}(\text{OCBu}'_3)]_2$ .<sup>9</sup> The structures observed for these compounds are associated with the degree of steric hindrance introduced by the pendant hydrocarbon chain of the alkoxide ligand. Using smaller, less sterically hindered ligands is an attractive means for obtaining alternative structural types, but the solubilities of the resultant  $[\text{Li}(\text{OR})]_n$  are often substantially reduced because of oligomerization (as noted for the OME derivative), which limits the utility of these compounds.

Recent investigations in our laboratory suggest that the ONep ligand has properties that are consistent with 2° and 3° alcohols.<sup>4,5,10–14</sup> For example, for the  $[\text{Ti}(\text{OR})_4]_n$  family, the 1° alkoxide (ethoxide<sup>15</sup> and methoxide<sup>16</sup>) derivatives have been isolated as the tetranuclear species  $[\text{Ti}_2(\mu_3\text{-OR})(\mu\text{-OR})_2(\text{OR})_5]_2$  with a molecular complexity (MC) of 2.4 in solution. The 2° isopropoxide (O-*i*-Pr) is an oil and has an MC = 1.4, whereas the 3° *tert*-butoxide is often reported as a mononuclear complex (MC = 1.0).<sup>17</sup> In contrast, the ONep derivative was isolated as the dinuclear species  $[\text{Ti}(\mu\text{-ONep})(\text{ONep})_3]_2$  with an MC = 1.0

(7) Wheatley, P. J. *J. Chem. Soc.* **1960**, 4270.(8) Williard, P. G.; MacEwan, G. J. *J. Am. Chem. Soc.* **1989**, *111*, 7671.(9) Beck, G.; Hitchcock, P. B.; Lappert, M. F.; Mackinnon, I. A. *J. Chem. Soc., Chem. Commun.* **1989**, 1312.(10) Boyle, T. J.; Alam, T. M.; Dimos, D.; Moore, G. J.; Buchheit, C. D.; Al-Shareef, H. N.; Mechenbeir, E. R.; Bear, B. R. *Chem. Mater.* **1997**, *9*, 3187.(11) Boyle, T. J.; Alam, T. M.; Mechenbeir, E. R.; Scott, B.; Ziller, J. W. *Inorg. Chem.* **1997**, *36*, 3293.(12) Boyle, T. J.; Pedrotty, D. M.; Scott, B.; Ziller, J. W. *Polyhedron* **1997**, *17*, 1959.(13) Boyle, T. J.; Alam, T. M.; Tafoya, C. J.; Scott, B. L. *Inorg. Chem.* **1998**, *37*, 5588.(14) Boyle, T. J.; Tyner, R. P.; Alam, T. M.; Scott, B. L.; Ziller, J. W.; Potter, B. G. *J. Am. Chem. Soc.* **1999**, *121*, 12104.(15) Ibers, J. A. *Nature (London)* **1963**, *197*, 686.(16) Wright, D. A.; Williams, D. A. *Acta Crystallogr., Sect. B* **1968**, *24*, 1107.

\* To whom correspondence should be sent.

- (1) Pauer, F.; Power, P. P. In *Lithium Chemistry. A Theoretical and Experimental Overview*; Sapse, A.-M., Schleyer, P. v. R., Eds.; John Wiley & Sons: New York, 1995; pp 295–392.
- (2) Sapse, A.-M.; Jain, D. C.; Rahgavachari, K. In *Lithium Chemistry. A Theoretical and Experimental Overview*; Sapse, A.-M., Schleyer, P. v. R., Eds.; John Wiley & Sons: New York, 1995; pp 45–66.
- (3) Boyle, T. J.; Pedrotty, D. M.; Alam, T. M.; Vick, S. C.; Rodriguez, M. A. *Inorg. Chem.* **2000**, *39*, 5133.
- (4) Boyle, T. J.; Bradley, D. C.; Hampden-Smith, M. J.; Patel, A.; Ziller, J. W. *Inorg. Chem.* **1995**, *34*, 5893.
- (5) Boyle, T. J.; Alam, T. M.; Tafoya, C. J.; Mechenbeir, E. R.; Ziller, J. W. *Inorg. Chem.* **1999**, *38*, 2422.
- (6) Zechmann, C. A.; Boyle, T. J.; Pedrotty, D. M.; Alam, T. M.; Lang, D. P.; Scott, B. L. *Inorg. Chem.* **2001**, *40*, 2177.

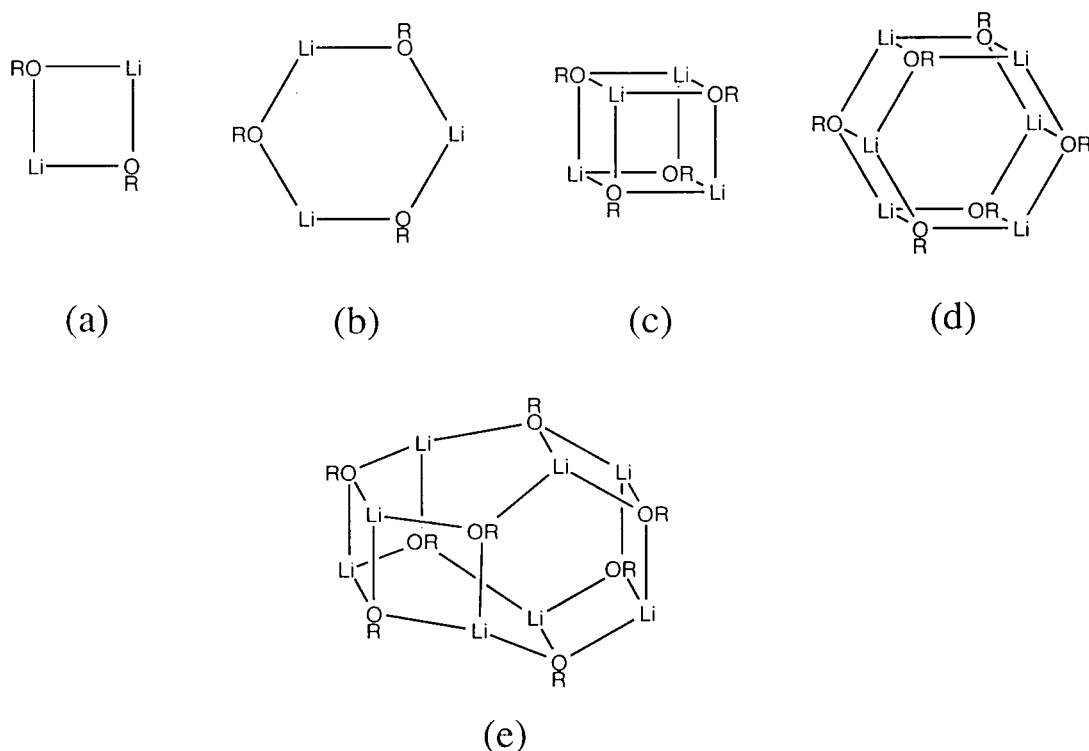


**Figure 1.** Schematic of Li(OR) structures: (a) hexagonal prism, (b) cube, (c) hexagon, (d) square, and (e) fused hexagon-cube prism.

in solution.<sup>11</sup> Therefore, it was of interest to determine the structural properties of Li(ONep) versus the other Li(OR) derivatives previously discussed.

This paper details the characterization of a series of Li(ONep) compounds isolated from a variety of solvents, including toluene from which  $[\text{Li}(\mu_3\text{-ONep})]_8$  (**1**), a unique structural arrangement for Li(OR) compounds, was isolated. From the more Lewis basic solvent systems tetrahydrofuran (THF) and pyridine (py),  $[\text{Li}(\mu_3\text{-ONep})]_4(\text{solvent})_3$  (solvent = THF (**2**) or py (**3**)) compounds were characterized. A comparison of the ONep ligated species to the aryloxide products will be discussed where appropriate.

### Experimental Section

All of the compounds were handled with the rigorous exclusion of air and water using standard Schlenk-line and glovebox techniques. All of the solvents were freshly distilled from the appropriate drying agent immediately prior to use.<sup>18</sup> The following chemicals were used as received (Aldrich), stored, and handled under an argon atmosphere:  $\text{LiN}(\text{SiMe}_3)_2$  and HONep.

All of the solid-state magic-angle spinning (MAS) NMR spectra were obtained at room temperature on a Bruker AMX-400 at 100.6, 155.5, and 58.9 MHz for  $^{13}\text{C}$ ,  $^7\text{Li}$ , and  $^6\text{Li}$ , respectively. A 4 mm broad-band (bb) MAS probe, spinning at 10–12.5 kHz, was used for all of the experiments. For  $^{13}\text{C}$ , 12.5 kHz was used to reduce the overlap between the spinning sidebands of the aromatic resonances with the other peaks of interest. The  $^{13}\text{C}$  cross-polarization (CP) MAS spectra were obtained using high-power  $^1\text{H}$  decoupling, 1 ms contact time, and 64–256 scan averages. The  $^{13}\text{C}$  spectra were referenced against the carbonyl resonance of external glycine ( $\delta$  176.0 with respect to TMS). The  $^6\text{Li}$  and  $^7\text{Li}$  MAS NMR spectra were obtained using single-pulse Bloch decay with high-power  $^1\text{H}$  decoupling and 64–256 scan averages and were referenced to either 1 M LiCl(aq) or 1 M  $^6\text{LiCl}$ (aq) ( $\delta = 0.0$ ). All of the  $^1\text{H}$ ,  $^7\text{Li}$ , and  $^{13}\text{C}$  solution-state NMR spectra were obtained on a Bruker DRX400 at 400.1, 155.4, and 100.1 MHz using a 5 mm

bb probe. FTIR data were obtained on a Bruker Vector 22 spectrometer using KBr pellets under an atmosphere of flowing nitrogen. Elemental analyses were performed on a Perkin-Elmer 2400 CHN-S/O elemental analyzer.

**General Synthesis.** In a flask, HONep was dissolved in the appropriate solvent and slowly added to a Schlenk flask containing  $\text{LiN}(\text{SiMe}_3)_2$  in the same solvent. After being stirred for 1 h, the reaction was a clear, pale-yellow solution. After 12 h, the volatile portion of the reaction mixture was removed in vacuo to yield a white powder. The powder redissolved in a minimal amount of the parent solvent and was placed at  $-25^\circ\text{C}$  or allowed to slowly evaporate at glovebox temperatures. The resultant crystals were acceptable for single-crystal X-ray analyses. Yields were not optimized.

**$[\text{Li}(\mu_3\text{-ONep})]_8$  (**1**).** HONep (18.5 g, 0.210 mol),  $\text{LiN}(\text{SiMe}_3)_2$  (35.1 g, 0.210 mol), and toluene (250 mL) were used. FTIR (KBr,  $\text{cm}^{-1}$ ): 2951 (s), 2864 (m), 2807 (m), 2691 (m), 2644 (w), 1479 (m), 1460 (w), 1399 (w), 1358 (m), 1251 (w), 1106 (s), 1087 (s), 1018 (m), 892 (w), 616 (s), 570 (m), 442 (m).  $^1\text{H}$  NMR (400.1 MHz, toluene- $d_8$ ):  $\delta$  3.80, 3.67 (1.9H, s,  $\text{OCH}_2\text{CMe}_3$ ), 1.02, 0.99 (9H, s,  $\text{OCH}_2\text{CMe}_3$ ).  $^{13}\text{C}\{^1\text{H}\}$  (100.1 MHz, toluene- $d_8$ ):  $\delta$  77.6 ( $\text{OCH}_2\text{CMe}_3$ ), 34.9 ( $\text{OCH}_2\text{CMe}_3$ ), 27.2, 26.8 ( $\text{OCH}_2\text{CMe}_3$ ).  $^7\text{Li}$  (155.4 MHz, toluene- $d_8$ ):  $\delta$  0.84. Anal. Calcd for  $\text{C}_5\text{H}_{11}\text{LiO}$ : C, 63.84; H, 11.78. Found: C, 63.51; H, 11.58.

**$[\text{Li}(\mu_3\text{-ONep})]_4(\text{THF})_3$  (**2**).** **Method A. General Synthesis.** HONep (18.5 g, 0.210 mol),  $\text{LiN}(\text{SiMe}_3)_2$  (35.1 g, 0.210 mol), and THF (250 mL) were used.

**Method B.** Compound **1** (1.00 g, 1.33 mmol) and THF (10 mL) were used. The reaction was stirred for 12 h, concentrated, and cooled to  $-25^\circ\text{C}$ . X-ray quality crystalline material was isolated and proved to be **2**. FTIR (KBr,  $\text{cm}^{-1}$ ): 2952 (s), 2865 (m), 2807 (m), 2778 (w), 2691 (m), 2645 (w), 1479 (m), 1461 (m), 1399 (m), 1358.2 (m), 1106 (s), 1086 (s), 1019 (m), 892 (w), 619 (s), 569 (s), 512 (m), 442 (m).  $^1\text{H}$  NMR (400.1 MHz, THF- $d_8$ ):  $\delta$  3.38 (1.9H, s,  $\text{OCH}_2\text{CMe}_3$ ), 0.81 (9H, s,  $\text{OCH}_2\text{CMe}_3$ ).  $^{13}\text{C}\{^1\text{H}\}$  (100.1 MHz, THF- $d_8$ ):  $\delta$  76.7 ( $\text{OCH}_2\text{CMe}_3$ ), 34.7 ( $\text{OCH}_2\text{CMe}_3$ ), 27.7 ( $\text{OCH}_2\text{CMe}_3$ ).  $^7\text{Li}$  (155.4 MHz, THF- $d_8$ ):  $\delta$  0.42. Anal. Calcd for  $\text{C}_{32}\text{H}_{68}\text{Li}_4\text{O}_7$ : C, 64.86; H, 11.57. Found: C, 63.42; H, 11.50.

**$[\text{Li}(\mu_3\text{-ONep})]_4(\text{py})_3$  (**3**).** **Method A. General Synthesis.** HONep (18.5 g, 0.210 mol),  $\text{LiN}(\text{SiMe}_3)_2$  (35.1 g, 0.210 mol), and py (250 mL) were used.

(17) Bradley, D. C.; Mehrotra, R. C.; Gaur, D. P. *Metal Alkoxides*; Academic Press: New York, 1978.

(18) Perrin, D. D.; Armarego, W. L. F. *Purification of Laboratory Chemicals*, 3rd ed.; Pergamon Press: New York, 1988.

**Table 1.** Data Collection Parameters for **1**

	compound		
	1	2	3
chemical formula	C <sub>40</sub> H <sub>88</sub> Li <sub>8</sub> O <sub>8</sub>	C <sub>32</sub> H <sub>68</sub> Li <sub>4</sub> O <sub>7</sub>	C <sub>35</sub> H <sub>59</sub> Li <sub>4</sub> N <sub>3</sub> O <sub>4</sub>
fw	752.62	592.62	613.61
temp (K)	168	168	168
space group	triclinic	triclinic	triclinic
crystal system	P1	P1	P1
<i>a</i> (Å)	10.622(2)	10.502(3)	10.552(4)
<i>b</i> (Å)	12.417(3)	10.507(3)	10.572(4)
<i>c</i> (Å)	20.960(4)	18.617(6)	10.724(4)
$\alpha$ (deg)	86.078(3)	86.200(5)	105.271(5)
$\beta$ (deg)	87.948(3)	79.263(5)	112.677(5)
$\gamma$ (deg)	74.079(3)	77.207(5)	101.756(5)
<i>V</i> (Å <sup>3</sup> )	2651.7(10)	1967.7(10)	1000.3(6)
<i>Z</i>	2	2	1
<i>D</i> <sub>calcd</sub> (mg/m <sup>3</sup> )	0.943	1.000	1.019
$\mu$ (mm <sup>-1</sup> )	0.060	0.066	0.064
R1 <sup>a</sup> (%)	5.20	7.82	6.72
wR2 <sup>b</sup> (%) [ <i>I</i> > 2 $\sigma$ ( <i>I</i> )]	12.71	22.27	16.63
R1 <sup>a</sup> (% , all data)	10.07	12.65	9.89
wR2 <sup>b</sup> (% , all data)	14.78	25.24	18.79

$$^a R1 = \sigma \left[ |F_o| - |F_c| \right] / \sigma |F_o|. \quad ^b wR2 = \left[ \sum [w(F_o^2 - F_c^2)^2] / \sum [w(F_o^2)^2] \right]^{1/2}.$$

**Method B.** Compound **1** (1.00 g, 1.33 mmol) and py (10 mL) were used. The reaction was stirred for 12 h, concentrated, and cooled to -25 °C. X-ray quality crystalline material was isolated and proved to be **3**. FTIR (KBr, cm<sup>-1</sup>): 2951 (s), 2902 (m), 2865 (s), 2811 (m), 2781 (m), 2703 (w), 2653 (m), 2611 (w), 1479 (m), 1460 (m), 1400 (m), 1359 (m), 1250 (w), 1215 (w), 1105 (s), 1083 (w), 1019 (m), 931 (w), 891 (w), 750 (w), 591 (s), 562 (s), 441 (s). <sup>1</sup>H NMR (400.1 MHz, py-*d*<sub>5</sub>):  $\delta$  3.85 (2H, s, OCH<sub>2</sub>CMe<sub>3</sub>), 1.02 (9H, s, OCH<sub>2</sub>CMe<sub>3</sub>). <sup>13</sup>C-<sup>1</sup>H (100.1 MHz, py-*d*<sub>5</sub>):  $\delta$  77.8 (OCH<sub>2</sub>CMe<sub>3</sub>), 37.9 (OCH<sub>2</sub>CMe<sub>3</sub>), 27.6 (OCH<sub>2</sub>CMe<sub>3</sub>). <sup>7</sup>Li (155.4 MHz, py-*d*<sub>5</sub>):  $\delta$  1.50. Anal. Calcd for C<sub>3</sub>H<sub>11</sub>LiO: C, 68.51; H, 9.69; N, 6.85. Found: C, 66.45; H, 10.17; N, 4.31.

**General X-ray Crystal Structure Information.**<sup>19</sup> A colorless crystal was mounted onto a thin glass fiber from a pool of Fluorolube and immediately placed under a liquid-N<sub>2</sub> stream on a Bruker AXS diffractometer. The radiation used was graphite monochromatized Mo K $\alpha$  radiation ( $\lambda = 0.710$  73 Å). The lattice parameters were optimized from a least-squares calculation on 48 carefully centered reflections. Lattice determination and data collection were carried out using SMART Version 5.054 software.<sup>19</sup> Data reduction was performed using SAINT+ Version 6.02 software.<sup>19</sup> The data were corrected for absorption using the program SADABS within the SAINT+ package.<sup>19</sup> The structures were solved in the appropriate space group (Table 1) using direct methods. This solution yielded Li, O, N, and some C atoms. Subsequent Fourier synthesis gave the remaining C-atom positions. The hydrogen atoms were fixed in positions of ideal geometry and refined within the XSHHELL software. These idealized hydrogen atoms had their isotropic temperature factors fixed at 1.2 or 1.5 times the equivalent isotropic *U* of the C atoms for which they were bonded. The final refinement included anisotropic thermal parameters on all of the non-hydrogen atoms and converged to the R1 and wR2 values listed in Table 1. Additional data collection parameters are listed in Table 1. Tables 2 and 3 list selected metrical data for compound **1** and compounds **2** and **3**, respectively.

## Results and Discussion

**Synthesis.** An amide–alcohol exchange (eq 1) reaction was used to generate the Li(ONep) compounds because of its simplicity and the high purity of the products. This was also the same method used to prepare the [Li( $\mu$ <sub>3</sub>-OAr)(solv)<sub>*x*</sub>]<sub>*n*</sub> family of compounds.<sup>3</sup> For **1–3**, LiN(SiMe<sub>3</sub>)<sub>2</sub> was dissolved in the appropriate solvent and HONep, predissolved in the same

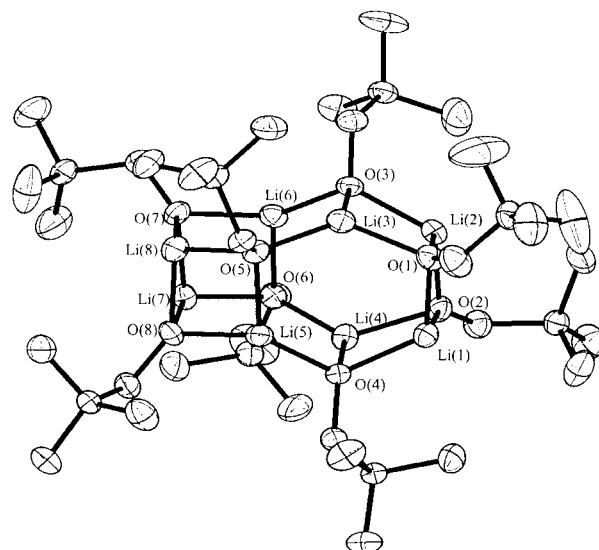
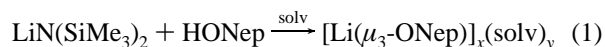


**Figure 2.** Thermal ellipsoid plot of **1**. Thermal ellipsoids are drawn at the 30% level.

solvent, was slowly added via pipet. The solvents investigated included toluene (tol), THF, and py.



solv = tol, *x* = 8, *y* = 0; solv = THF or py, *x* = 4, *y* = 3

In toluene, both of the precursors slowly dissolved over time while being stirring. After 12 h, the volatile fraction of the reaction was removed, and the resulting powder was redissolved in toluene. Crystals of **1** were grown by either slow evaporation or cooling of a saturated solution. The analytical data of the crystals and the bulk powder were identical. Figure 2 is a thermal ellipsoid plot of **1**. Compound **1** was found to be very soluble in toluene. The elemental analysis of **1** is consistent with the observed solid-state structure. The FTIR spectrum of **1** reveals standard ONep stretches with an absence of the OH stretch indicative of complete reaction with no residual HONep being present.

Following the above synthesis but replacing toluene with THF or py (or by redissolving **1** in the appropriate Lewis basic solvents) led to the isolation of [Li( $\mu$ <sub>3</sub>-ONep)]<sub>4</sub>(solv)<sub>3</sub> (solv = THF (**2**) or py (**3**)). Figures 3 and 4 are the thermal ellipsoid plots of **2** and **3**, respectively. The elemental analyses of **2** and **3** were low in total composition percentages. This variation was observed for other solvated Li(OR)(solv) species and is typically due to the preferential loss of solvent.<sup>3</sup> The FTIR spectra of **2** and **3** differ from that of **1** in the addition of stretches consistent with the solvent utilized.

**Solid State. (a) Compound 1.** The structure of **1**, shown in Figure 2, is a novel arrangement for Li(OR) compounds. It consists of alternating Li and O (as part of the ONep ligand) atoms forming an eight-membered ring prism. Because of an internal Li–O bond, the eight-membered ring resembles a fused hexagon–square. Where the cube and hexagon are joined, the top and bottom Li and O atoms are puckered away from each other. These Li–O distances are too long to be formally considered a bond [Li(3)–O(4) = 3.408 Å, Li(4)–O(3) = 3.384 Å, Li(5)–O(6) = 3.465 Å, Li(6)–O(5) = 3.397 Å]. This leaves the molecule as a dual-fused fused hexagon–square, where each Li atom adopts a three-coordinated distorted pyramidal geometry. A schematic drawing is shown in Figure 1e, and the thermal ellipsoid plot is shown in Figure 2. The symmetry of the

(19) The listed versions of SAINT, SMART, XSHHELL, XPow in SHELXTL, and SADABS software from Bruker Analytical X-ray Systems Inc., Madison, WI, were used in the analyses.

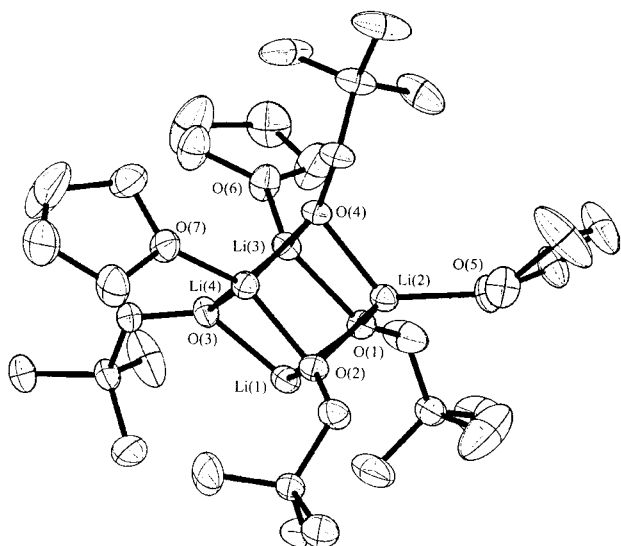


**Figure 3.** Thermal ellipsoid plot of **2**. Thermal ellipsoids are drawn at the 30% level.

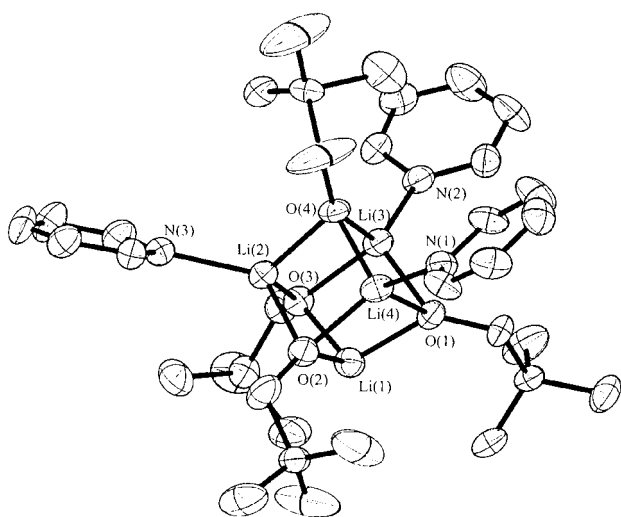


**Figure 4.** Thermal ellipsoid plot of **3**. Thermal ellipsoids are drawn at the 30% level.

molecule yields two types of nonequivalent Li and ONep ligands. The metrical data of **1** are tabulated in Table 2 (av Li–ONep = 1.89 Å; Li–Li = 2.41–3.26 Å; Li–O–Li = 79.67–120.5°; O–Li–O = 96.51–128.2°). The distances are significantly shorter than what was reported for the  $[\text{Li}(\text{OAr})(\text{THF})_x]_n$  complexes but are in agreement with the py adducts  $[\text{Li}(\text{OAr})(\text{py})_x]_2$ .<sup>3</sup> The angles of **1** cover a larger range than those noted for the OAr derivatives. These metrical phenomena must be attributed to the lack of electron donation by the Lewis basic solvent because the metrical data of **2** and **3** (see Table 3) are similar to that of the  $[\text{Li}(\text{OAr})(\text{solv})_x]$  compounds.<sup>3</sup>

In an effort to verify that the bulk sample was consistent with the observed solid-state structure, solid-state <sup>6,7</sup>Li and <sup>13</sup>C MAS NMR spectra were collected for **1**. In the solid state, the <sup>6</sup>Li NMR chemical shift is equal to the true isotropic chemical shift (because the second-order quadrupolar shift is negligible for <sup>6</sup>Li) and is used to discuss changes in structure. The Li chemical shift is a function of the local environment around the metal and is influenced by both the number of neighboring coordinating anions and their respective distances. Secondary effects on the observed Li chemical shift resulting from the nature and spatial arrangement of the surrounding cations within the

**Table 2.** Selected Distances and Angles for **1**

Li–O	distances (Å)	Li–Li	distances (Å)
Li(1)–O(1)	1.875(5)	Li(1)–Li(2)	2.426(6)
Li(1)–O(2)	1.869(5)	Li(1)–Li(3)	3.045(6)
Li(1)–O(4)	1.872(4)	Li(1)–Li(4)	2.411(6)
Li(2)–O(1)	1.884(5)	Li(1)–Li(5)	3.239(6)
Li(2)–O(2)	1.869(5)	Li(2)–Li(3)	2.451(6)
Li(2)–O(3)	1.886(5)	Li(2)–Li(4)	2.979(6)
Li(3)–O(1)	1.886(5)	Li(2)–Li(6)	3.243(6)
Li(3)–O(3)	1.905(5)	Li(3)–Li(5)	2.927(6)
Li(3)–O(5)	1.858(4)	Li(3)–Li(6)	2.975(6)
Li(4)–O(2)	1.903(4)	Li(3)–Li(8)	3.265(6)
Li(4)–O(4)	1.934(5)	Li(4)–Li(5)	2.969(6)
Li(4)–O(6)	1.840(5)	Li(4)–Li(6)	2.965(6)
Li(5)–O(4)	1.863(4)	Li(4)–Li(7)	3.181(6)
Li(5)–O(5)	1.943(4)	Li(5)–Li(8)	2.499(6)
Li(5)–O(8)	1.894(5)	Li(5)–Li(7)	3.046(6)
Li(6)–O(3)	1.857(5)	Li(6)–Li(7)	2.442(6)
Li(6)–O(6)	1.920(4)	Li(6)–Li(8)	2.971(6)
Li(6)–O(7)	1.906(5)	Li(7)–Li(8)	2.412(6)
Li(7)–O(6)	1.872(4)		
Li(7)–O(7)	1.892(4)		
Li(7)–O(8)	1.884(5)		
Li(8)–O(5)	1.902(5)		
Li(8)–O(7)	1.863(5)		
Li(8)–O(8)	1.882(4)		

( $\mu_3$ -O)–Li–( $\mu_3$ -O)	angles (deg)	Li–( $\mu_3$ -O)–Li	angles (deg)
O(1)–Li(1)–O(4)	117.2(2)	Li(1)–O(1)–Li(2)	80.41(19)
O(2)–Li(1)–O(4)	102.2(2)	Li(1)–O(1)–Li(3)	108.11(19)
O(2)–Li(1)–O(1)	99.2(2)	Li(2)–O(1)–Li(3)	108.11(19)
O(1)–Li(2)–O(3)	99.1(2)	Li(2)–O(2)–Li(1)	81.0(2)
O(2)–Li(2)–O(3)	120.7(2)	Li(2)–O(2)–Li(4)	104.30(19)
O(2)–Li(2)–O(1)	98.8(2)	Li(1)–O(2)–Li(4)	79.46(19)
O(5)–Li(3)–O(1)	127.8(2)	Li(6)–O(3)–Li(2)	120.1(2)
O(5)–Li(3)–O(3)	121.6(2)	Li(6)–O(3)–Li(3)	104.53(19)
O(1)–Li(3)–O(3)	98.4(2)	Li(2)–O(3)–Li(2)	80.5(2)
O(6)–Li(4)–O(2)	125.1(2)	Li(5)–O(4)–Li(1)	120.3(2)
O(6)–Li(4)–O(4)	125.3(2)	Li(5)–O(4)–Li(4)	112.12(19)
O(2)–Li(4)–O(4)	98.7(2)	Li(1)–O(4)–Li(4)	102.9(2)
O(4)–Li(5)–O(8)	123.6(2)	Li(3)–O(5)–Li(8)	120.5(2)
O(4)–Li(5)–O(5)	125.7(2)	Li(3)–O(5)–Li(5)	100.68(19)
O(8)–Li(5)–O(5)	96.51(19)	Li(8)–O(5)–Li(5)	81.07(19)
O(3)–Li(6)–O(7)	128.2(2)	Li(4)–O(6)–Li(7)	118.0(2)
O(3)–Li(6)–O(6)	121.4(2)	Li(4)–O(6)–Li(6)	104.11(19)
O(7)–Li(6)–O(6)	97.93(19)	Li(7)–O(6)–Li(6)	80.16(19)
O(6)–Li(7)–O(8)	120.4(2)	Li(8)–O(7)–Li(7)	79.93(19)
O(6)–Li(7)–O(7)	100.1(2)	Li(8)–O(7)–Li(6)	104.0(2)
O(8)–Li(7)–O(7)	99.2(2)	Li(7)–O(7)–Li(6)	79.99(18)
O(7)–Li(8)–O(8)	100.4(2)	Li(8)–O(8)–Li(7)	79.67(19)
O(7)–Li(8)–O(5)	121.5(2)	Li(8)–O(8)–Li(5)	82.88(19)
O(8)–Li(8)–O(5)	98.4(2)	Li(7)–O(8)–Li(5)	107.44(19)

structure have also been noted.<sup>3,20,21</sup> The chemical shift range for <sup>6,7</sup>Li NMR is quite small (<10 ppm).<sup>3,20,21</sup>

One peak was observed for the <sup>6</sup>Li MAS spectrum of **1** at  $\delta$  0.51 (the frequency of the maximum peak is recorded in Table 4). The <sup>6</sup>Li MAS NMR chemical shift for other three-coordinated Li atoms of the  $[\text{Li}(\text{OAr})(\text{solv})_x]_n$  family, OAr = OPh ( $\delta$  0.58 and –0.11), DIP ( $\delta$  0.41), and DBP ( $\delta$  0.51), had similar chemical shifts (the two distinct signals observed for the OPh derivative were attributed to the presence of multiple structural types). The observed resonance for **1** was asymmetric and could be deconvoluted into two overlapping resonances in an ~1:4 ratio. As mentioned before, the solid-state structure of **1** possesses two types of three-coordinated Li atoms in a 1:1 ratio: four internal [Li(3), Li(4), Li(5), Li(6)] and four external [Li(1), Li(2), Li(7), Li(8)]. The internal Li cations adopt a much

(20) Xue, X.; Stebbins, J. F. *Phys. Chem. Miner.* **1993**, *20*, 297.

(21) Alam, T. M.; Conzone, S.; Brow, R. K.; Boyle, T. J. *J. Non-Cryst. Solids* **1999**, *258*, 140.

**Table 3.** Selected Distances and Angles for **2** and **3**

Distances (Å)			
<b>2</b>		<b>3</b>	
Li-O			
Li(1)-O(1)	1.895(7)	Li(1)-O(1)	1.847(11)
Li(1)-O(2)	1.867(7)	Li(1)-O(2)	1.875(12)
Li(1)-O(3)	1.873(6)	Li(1)-O(3)	1.877(11)
Li(2)-O(1)	1.934(6)	Li(2)-O(1)	1.992(11)
Li(2)-O(2)	1.947(7)	Li(2)-O(2)	1.905(12)
Li(2)-O(4)	1.930(6)	Li(2)-O(4)	1.924(10)
Li(3)-O(1)	1.967(6)	Li(3)-O(1)	1.930(10)
Li(3)-O(3)	1.930(6)	Li(3)-O(3)	1.994(11)
Li(3)-O(4)	1.965(6)	Li(3)-O(4)	1.923(11)
Li(4)-O(2)	1.959(6)	Li(4)-O(2)	1.976(10)
Li(4)-O(3)	1.963(6)	Li(4)-O(3)	1.893(11)
Li(4)-O(4)	1.925(6)	Li(4)-O(4)	1.931(11)
Li-solv			
Li(2)-O(5)	1.984(6)	Li(2)-N(1)	2.082(12)
Li(3)-O(6)	1.981(6)	Li(3)-N(2)	2.062(11)
Li(4)-O(7)	1.982(6)	Li(4)-N(3)	2.073(11)
Li-Li			
Li(1)-Li(4)	2.518	Li(1)-Li(2)	2.464
Li(1)-Li(2)	2.477	Li(1)-Li(3)	2.487
Li(1)-Li(3)	2.473	Li(1)-Li(4)	2.482
Li(2)-Li(3)	2.563	Li(2)-Li(3)	2.572
Li(2)-Li(4)	2.559	Li(2)-Li(4)	2.541
Li(3)-Li(4)	2.577	Li(3)-Li(4)	2.554
Angles (deg)			
<b>2</b>		<b>3</b>	
$(\mu_3\text{-O})\text{-Li-}(\mu_3\text{-O})$			
O(2)-Li(1)-O(1)	100.4(3)	O(2)-Li(1)-O(1)	101.7(6)
O(2)-Li(1)-O(3)	101.3(3)	O(2)-Li(1)-O(3)	101.6(5)
O(2)-Li(2)-O(1)	96.2(3)	O(2)-Li(2)-O(1)	95.6(5)
O(1)-Li(2)-O(4)	98.4(3)	O(1)-Li(2)-O(4)	95.6(5)
Li- $(\mu_3\text{-O})$ -Li			
Li(1)-O(2)-Li(2)	81.0(3)	Li(1)-O(2)-Li(2)	81.4(5)
Li(1)-O(2)-Li(4)	82.3(3)	Li(1)-O(2)-Li(4)	80.2(4)
Li(2)-O(2)-Li(4)	81.9(3)	Li(2)-O(2)-Li(4)	81.8(4)
Li(2)-O(4)-Li(4)	83.2(3)	Li(2)-O(4)-Li(4)	82.5(4)
solv-Li- $(\mu_3\text{-O})$			
O(5)-Li(2)-O(1)	132.8(3)	N(1)-Li(2)-O(1)	112.2(5)
O(5)-Li(2)-O(2)	111.8(3)	N(1)-Li(2)-O(2)	134.2(6)

**Table 4.** Solid-State MAS NMR Data for **1-3**

compd	$^{13}\text{C}$ (ppm)	$^6\text{Li}$ MAS <sup>a</sup> (ppm)	$^7\text{Li}$ MAS <sup>a</sup> (ppm)	$^7\text{Li}$ $P_Q$ <sup>b</sup> (kHz)
<b>1</b>	76.6 (OCH <sub>2</sub> CM <sub>3</sub> )	0.51(5)	0.4(1)	80
	33.9 OCH <sub>2</sub> CM <sub>3</sub> )			
	27.1 (OCH <sub>2</sub> CM <sub>3</sub> )			
<b>2</b>	77.4 (THF)	0.53(5)	0.5(1)	80
	76.5 (OCH <sub>2</sub> CM <sub>3</sub> )			
	33.9 (OCH <sub>2</sub> CM <sub>3</sub> )			
	27.1 (OCH <sub>2</sub> CM <sub>3</sub> )			
	26.1 (THF)			
<b>3</b>	148.8 (py)	1.08(5), 0.60(5)	0.6(2)	280
	135.6 (py)			
	123.7 (py)			
	78.8, 76.3 (OCH <sub>2</sub> CM <sub>3</sub> )			
	34.8, 33.3 (OCH <sub>2</sub> CM <sub>3</sub> )			
	26.3, 24.3 (OCH <sub>2</sub> CM <sub>3</sub> )			

<sup>a</sup> Peak maximum, not corrected for quadrupolar shift effects.

<sup>b</sup> Quadrupolar coupling product was estimated from the width of the spinning sideband manifold and has an error of about  $\pm 10$  kHz.

more planar geometry than that noted for the external Li atoms. If the variations of these Li atoms are significant enough, then this would explain the two  $^6\text{Li}$  resonances, but the ratio is not consistent. An alternative explanation may be the presence of two types of structural species as noted for the OPh derivatives

(vide infra). Therefore, additional nuclei were investigated to clarify the source of the two resonances noted for **1** (inequivalent Li atoms or multiple structure types).

The  $^7\text{Li}$  MAS NMR spectrum of **1** revealed only a single resonance at 0.4 ppm. This shift is consistent with those observed for the four-coordinated Li of the phenoxide ( $\delta$  0.2, OPh) and the three-coordinated Li of 2,6-di-*tert*-butyl phenoxide ( $\delta$  0.1, DBP) complexes that adopt a cube (Figure 1d) and square (Figure 1a) structure, respectively. The only other three-coordinated Li atom complex in the previous study, 2,6-diisopropyl phenoxide (DIP), had a resonance at 0.5 ppm. It is of note that, for the aryloxy derivatives, THF solvent molecules fill the coordination sphere and will effect the final chemical shift to some degree because of the electron donation of these compounds.  $^7\text{Li}$  MAS NMR spectra are typically broad,<sup>3,20,21</sup> resulting in a loss of spectral resolution which precludes the observation of inequivalent Li environments as was noted in the  $^6\text{Li}$  MAS NMR spectrum. The quadrupolar coupling product (also known as SOQE or QSC) is defined by  $P_Q = C_q(1 + \eta_Q^{2/3})^{1/2}$ , where  $C_Q = e^2qQ/h$  is the quadrupolar coupling constant and  $\eta_Q$  is the quadrupolar electrical field gradient asymmetry parameter.<sup>3</sup> The parameter  $P_Q$  can be used as a measure of an indication of the asymmetry of the electrical field gradient around the Li atoms, wherein a larger  $P_Q$  value indicates a lower symmetry. For the OAr derivatives, it was noted that  $P_Q$  values below 150 kHz were consistent with four-coordinated Li metal centers and that those above 250 kHz were in agreement with three-coordinated Li metal centers.<sup>3</sup> For **1**, the  $P_Q$  value of 85 is indicative of a symmetric environment, which is not in agreement with the three-coordinated Li atoms observed in the crystal structure (Figure 2). While the Li-O distances for these compounds (av Li-O = 3.44 Å) are too long to be considered bonded, some influence must be present, and this forced interaction may place the Li atom in a pseudotetrahedral environment, yielding the lower  $P_Q$  value. Alternatively, the lack of solvation may also impact the  $P_Q$  value, rendering previously observed trends with solvated species invalid for unsolvated complexes such as **1**.<sup>3</sup> The  $^{13}\text{C}$  MAS spectrum revealed a single set of resonances consistent with ONep components (methylene, quaternary, and methyl). Combined, the data discussed previously are inconclusive concerning the exact structure of the bulk powder.

Because of the similarity of the various cationic environments, it is difficult to distinguish the minor variations noted for the solid-state structure. Therefore, several crystals (<5) were selected for single-crystal structure analyses, and all of these proved to have the same structure as that noted for **1**. Furthermore, using the data collected for the single-crystal X-ray structure, a powder XRD pattern was generated<sup>19</sup> and can be found in the Supporting Information. The bulk powder was heat-sealed in an airtight plastic envelope, and an XRD pattern was collected for **1**. In general, the calculated and observed powder diffraction patterns were in agreement, indicating that the bulk powder consisted mainly of the same constructs as those observed in the single-crystal structure. The experimental pattern did have peaks with varying intensities when compared to the calculated pattern, but this is not unexpected because of the difficulties in obtaining a truly randomized powder by our techniques.

It is of interest to know if the solid-state structure is retained in solution. Crystals of **1** were dried and redissolved in toluene-*d*<sub>8</sub>. Again, for the retention of the solid-state structure, two types of ONep and Li atoms should be observed. The solution-state multinuclear NMR data revealed only one set of ONep

resonances for the  $^{13}\text{C}$  and  $^1\text{H}$  spectra and a single  $^7\text{Li}$  resonance at 0.49 ppm. The use of other solvents could be used to further elucidate structural information. For the  $\text{Li}(\text{OAr})(\text{solv})$  family, Lewis basic solvents, THF or py, were used to determine their solution behavior. If one of these solvents is used, compound **1** will be transformed into either **2** or **3** and, thus, will not aid in the identification of the solution behavior of these compounds. Because the  $^7\text{Li}$  NMR solution and solid-state chemical shifts of **1** are consistent with each other, it is implied that the solid- and solution-state structures possess nearly identical arrangements. The single set of  $^{13}\text{C}$  and  $^7\text{Li}$  resonances in solution is, as is often noted for metal alkoxide complexes, a result of ligand scrambling.

**(b) Compounds 2 and 3.** Figures 3 and 4 show the thermal ellipsoid plots of the structures of **2** and **3**, respectively. Each of these compounds adopts a cubic structure, wherein one of the Li atoms does not coordinate a solvent molecule. This undersolvation was previously noted for the  $[\text{Li}(\text{OC}_6\text{H}_2(\text{Me})_3-2,4,6)(\text{THF})_4]$  derivative.<sup>22</sup> It is not fully understood why this species should be undersolvated when the sterically similar  $[\text{Li}(\text{OC}_6\text{H}_3(\text{Me})_2-2,6)(\text{THF})_4]$  derivative was found to be fully solvated. The *p*-methyl group does not increase the electron donation by the ring, as noted by the standard Li–O distances for the  $[\text{Li}(\text{OC}_6\text{H}_3(\text{Me})_2-2,6)(\text{THF})_4]$  complex.<sup>22</sup> In contrast to the OAr complexes, the Li atoms for **2** and **3** would be more electropositive because of decreased electron donation by the aliphatic versus aromatic ligand and should favor increased solvation. Thus, the steric hindrance by the ONep ligand must be used to explain the lack of solvation noted for **2** and **3**. Inspection of the solid-state structure reveals that the ONep ligands preferentially point in the same direction and that the *tert*-butyl groups effectively isolate one of the Li atoms, preventing solvation. The metrical data of **2** and **3** (see Table 3) are consistent with the OAr cubic analogues with Li–( $\mu_3$ -ONep) distances of av 1.94 and 1.92 Å, respectively, and Li–Li distances of av 2.53 and 2.52 Å, respectively. The Li–O–Li angles are  $\sim 81^\circ$ , and the O–Li–O angles are around  $90^\circ$  for both compounds.

For the solid-state structure of **2** and **3**, because of the  $C_3$  axis of rotation in the molecule, there is a 3:1 ratio for the two types of ONep ligands and two types of Li atoms (three of which are four-coordinated and one of which is three-coordinated). The  $^6\text{Li}$  MAS NMR spectrum of **2** has only one peak, whereas the  $^6\text{Li}$  MAS NMR spectrum for **3** indicates that two types of Li atoms are present (see Table 4). The latter spectrum is consistent with the solvated versus unsolvated Li environments. The variation between the structurally similar compounds may be explained by the strength of the Lewis basic solvent. Because py is more basic than THF, sufficient electron donation by py to illuminate the inequivalent environments may occur. An alternative explanation would be the presence of two structure types for **3**. The XRD powder patterns of **2** and **3** were compared to the calculated pattern.<sup>19</sup> While the resulting spectra were broader and the ratio of peaks varied, the majority of the pattern was in agreement, which implies the presence of only one compound in the bulk powder for both **2** and **3**.

Further investigations were undertaken using alternative NMR nuclei. The single environment of  $^7\text{Li}$  CP MAS indicates only one structure type present for each sample. Therefore, the electronic influence of py must be reinforcing the solvated versus unsolvated environments noted for the solid-state  $^6\text{Li}$  NMR spectrum. The  $^{13}\text{C}$  MAS NMR spectrum of **2** had only one set

of ONep and THF ligand resonances, whereas, for **3**, one set of py resonances is observed but two sets of ONep ligand resonances are present. Again, the strength of the py solvent must be reinforcing the disparity between the metal centers.

The  $P_Q$  value of the tetrahedral Li atoms of **2** was calculated and found to be in agreement with the values noted for the tetrahedral Li atom of the OAr derivatives. This is not unexpected because the THF/cube structure was what was previously noted for the OAr derivatives.<sup>3</sup> However,  $P_Q$  of the tetrahedral Li atoms of **3** (cube/py) does not follow the previous trend. The influence of py for the Li atoms of the cube structure must alter the observed  $P_Q$  values. This cube arrangement was not previously noted for the  $[\text{Li}(\text{OAr})(\text{py})_x]_2$  derivatives.<sup>3</sup> This observation suggests that the strength of the solvent coordinated must be taken into account, along with the coordination geometry, when interpreting the  $P_Q$  values. An increased number of structurally characterized solvated species with varied structure types will be required to fully understand the structural and coordination properties that influence  $P_Q$ .

Crystals of **2** and **3** were dried and redissolved in their parent solvent to investigate their solution behavior. The solution-state  $^1\text{H}$ ,  $^7\text{Li}$ , and  $^{13}\text{C}$  NMR data reveal only one set of resonances. The  $^7\text{Li}$  resonance of  $\delta$  0.8 for **2** is consistent with a cubic structure. For **3**, there were no reported cubic py adducts, therefore, it is difficult to make any comparisons, but the shift of 1.50 ppm is much further upfield than the dinuclear species isolated for the OAr derivatives.<sup>3</sup> On the basis of the data collected on these species and comparisons to other  $\text{Li}(\text{OAr})(\text{solv})_x$  cube structures, it appears that **2** and **3** retain their structures in solution; however, the extent of solvation that these molecules retain is not clear.

## Summary and Conclusion

The structure of  $[\text{Li}(\mu_3\text{-ONep})]_8$  (**1**), an unsolvated hexagon–cube prismatic structure, is novel in comparison to the previously characterized  $\text{Li}(\text{OR})$  compounds. Even with the increased nuclearity in comparison to the OAr derivatives, the unsolvated species **1** maintains a high degree of solubility. Solution studies are not conclusive but imply that the structure of **1** is retained in solution. Synthesizing  $\text{Li}(\text{ONep})$  in the presence of a Lewis base yields a standard cube structure,  $[\text{Li}(\mu_3\text{-ONep})]_4(\text{solv})_3$ , with only three of the Li atoms coordinating the solvent. XRD patterns and solid-state NMR data of **1–3** indicate that the single-crystal structures and the bulk powder were consistent. It was noted from the CP MAS data that the trends previously observed for the  $P_Q$  values of the  $\text{Li}(\text{OAr})(\text{solv})_x$  do not hold for these compounds.<sup>3</sup> The structural effect on  $P_Q$  must involve additional variables besides the coordination environment of the atom of interest, such as the polarity (i.e., the strength of the coordinated solvent) of the various bonds. The solution studies on these molecules indicate the retention of the solid-state structure, with ligand scrambling occurring. As noted previously, the ONep ligand continues to yield complexes with structure types that are not in line with other members of the family.

**Acknowledgment.** For support of this research, the authors thank the Office of Basic Energy Science and the U.S. Department of Energy under Contract DE-AC04-94AL85000. Sandia is a multiprogram laboratory operated by Sandia Corporation, a Lockheed Martin Company, for the United States Department of Energy.

**Supporting Information Available:** X-ray crystallographic files of **1–3** in CIF format. This material is available free of charge via the Internet at <http://pubs.acs.org>.

(22) Thiele, K.; Goerls, H.; Seidel, W. Z. *Anorg. Allg. Chem.* **1998**, 624, 1391.